CONFINEMENT AND THE PARTON MODEL IN TWO-DIMENSIONAL QCD

By J. H. Weis*†

CERN — Geneva and University of Washington, Seattle**

(Presented at the XVIII Cracow School of Theoretical Physics, Zakopane, May 26 — June 8, 1978)

Two-dimensional QCD is studied as a model for the possible effects of confinement on the predictions of the naive parton model which is based on the free propagation of quark--partons. We find that in processes involving large momentum transfers the naive parton model scaling laws are generally true even though quarks cannot be treated as propagating freely. The universality of quark fragmentation does not extend, however, to hadron-hadron scattering at small momentum transfers. Confinement strongly influences the probability of finding a "wee" quark in a hadron and this leads to a number of interesting consequences

1. Introduction

The quark-parton model [1] has come to play a central role in our thinking about processes involving hadrons. Originally the parton model was introduced to provide a physical picture for processes controlled by the behaviour of hadronic matter at very short distances: namely, the total cross-sections for e^+e^- annihilation into hadrons ($\gamma^* \to X$) and for deep inelastic scattering ($\gamma^* h \to X$). Although only for these processes can the parton model be rigorously derived from the short-distance behaviour of field theory, it has since been applied to many other processes with phenomenological success.

The basic idea of the naive parton model used in its many applications is that the basic interaction responsible for a given process takes place between elementary partons and the effects of the binding of partons into physical hadrons can be entirely expressed through phenomenological parton distribution functions. Thus, for example, the single--particle inclusive cross-section for deep inelastic scattering ($\gamma^* h \to h'X$) is described by the simple parton model diagram shown in Fig. 1. In the appropriate kinematic region (see Section 3.2), the cross-section is given in terms of the probabilities for finding parton a in hadron h and hadron h′ in parton a and the pointlike electron-parton cross-section. While the large momentum transfer subprocess of electron-parton scattering is involved and thus hadronic matter is probed at short distances as in the case of the total deep inelas-

* A. P. Sloan Foundation Fellow.

† Deceased

** Address: Physics Department, University of Washington, Seattle, WA 98105, USA.

tic cross-section, long-distance effects can also play an important role: the final state hadron h′ emerges after the long-range confining force has acted between parton a and the remaining constituents of h. In many of the other applications of the parton model which are not rigorously derivable from the short-distance behaviour of field theory

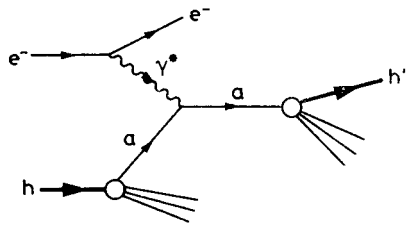

Fig. 1. Naive parton model diagram for $\gamma^* h \to h'X$

(e. g., the single-particle inclusive e^+e^- annihilation cross-section ($\gamma^* \to hX$), large mass lepton-pair production in hadron collisions ($hh' \to \gamma^* X$), and large transverse momentum processes in hadron-hadron collisions) the situation is similar: although a large momentum transfer subprocess is involved, in principle long-distance effects can be important. Parton model ideas have also been applied to hadron-hadron collisions involving no large momentum transfers; for example, to relate Regge behaviour to the probability of finding a "wee" parton in a hadron [1] and to make models for inclusive single-particle spectra [2].

Given the fruitfulness of the naive parton model it now seems like a good time to refine and extend our understanding of its predictions and its range of application. One can envision corrections to the naive parton model arising from both the extremes of (*i*) large

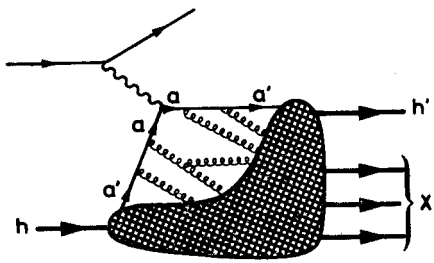

Fig. 2. Parton model diagram for $\gamma^* h \to h'X$ indicating short- and long-distance effects

momentum transfer (short-distance) effects and (*ii*) small momentum transfer (long-distance) effects. Since it now seems a good possibility that hadrons are described by quantum chromodynamics (QCD) which is a theory which is only asymptotically free, the naive parton model scaling laws must be corrected for large momentum transfer effects. On the other hand, since partons (quarks and gluons) appear to be confined inside hadrons, their interactions at long distances are very strong and the naive parton model may require modifications or limitations of its domain of applicability due to long-distance effects as we have already alluded to in the preceding paragraph. These two types of effects are indicated schematically in the modified form of Fig. 1 for $\gamma^* h \to h'X$ shown in Fig. 2. The modifications at short distances due to asymptotic freedom are indicated by the emission

of gluons which degrade the momenta of the quarks. The effects of long distances and confinement are indicated by the large shaded region from which the hadron h′ emerges.

The treatment of the short distance modifications of the parton model has been the subject of considerable interest recently and will be discussed by other lecturers [3]. I will discuss the other extreme — the possible effects of long-distance phenomena and especially quark confinement on the naive quark-parton model. It seems to be a common assumption that the short- and long-distance modifications of the parton model can be treated separately and combined together at the end, although there is as yet certainly no proof of this and, at least to me, it is by no means obvious. However, it is useful, even necessary, with our present limited level of understanding to adopt this assumption.

Since as yet the mechanism of confinement in QCD in the real world of four space--time dimensions is poorly understood, I will discuss QCD in one space and one time dimension (QCD_2) as a model for quark confinement [4]. This model has both the "short" distance ("hard") properties which motivated the naive parton model and the long-distance ("soft") properties which are characteristic of composite-Reggeized hadrons. It is thus an ideal model (indeed it is the only model *known* to possess both standard hard and soft physics) in which to study the relationship between confinement and the parton model. Although the mechanism of confinement is entirely different than in QCD in four dimensions, we may hope that the qualitative consequences of confinement are rather similar. Indeed I believe the reader will find it rather plausible that the general conclusions we draw are general features of confinement.

In Section 2, I review some salient features of QCD_2. For a more detailed discussion the reader is referred to the lectures of Ellis [5]. I will endeavour, however, to keep the presentation self-contained and where possible illustrate points with simple low order perturbation theory calculations. Some comments on gauge invariance in QCD_2 are relegated to an Appendix. In Section 3, I first discuss how the processes rigorously dominated by short distances are realized in QCD_2, i. e., verify that the physical final state hadrons give the same cross-sections "as if" free quarks were produced. Then I discuss other processes to which the parton model has been traditionally applied and compare the results in QCD_2 with the naive parton model. Finally, in Section 4, I summarize the results of Section 3 and discuss the lessons about the validity of the naive parton model that one is tempted to draw from these results.

2. *Review of two-dimensional QCD*

From an examination of the standard QCD Lagrangian one sees that the gluon coupling constant g has dimensions $[g] = L^{-1}$ in two dimensions. Thus the colour Coulomb potential between two quarks ($[V \propto g^2 r^n] = L^{-1}$) must grow linearly with distance ($n = 1$) and is therefore confining. In addition the theory is super-renormalizable and in the deep Euclidean region ($p^2 \to -\infty$) the lowest order graphs dominate since higher order graphs behave like $(g^2/p^2)^N$. This guarantees the validity of the exact scaling laws of the naive parton model for spacelike momenta for the short-distance dominated processes. The model is thus quickly seen to have the two features in which we are interested.

Since the gluon field has no transverse components, it has no independent degrees of freedom in two dimensions. Therefore, we cannot study two-dimensional analogues of processes associated with gluons (gluonium) or gluon jets. In fact, the absence of gluon emission is related to the existence of exact scaling in QCD_2 as opposed to the logarithmic violations characteristic of asymptotic freedom. Indeed gluon exchange in two dimensions is analogous to an "effective" confining potential in four dimensions rather than to the gluon state. The interest in QCD_2 is not so much in the fact that it is the two-dimensional version of most people's favourite theory in four dimensions but instead in the fact that it has the properties of confinement and scaling.

2.1. The $1/N_c$ expansion

An expansion in $1/N_c$ with g^2N_c fixed has very interesting properties in a confining theory with $SU(N_c)$ colour symmetry [6, 7]. The leading order term has zero-width resonances and is analogous to the dual resonance model while higher order terms generate the dual loop expansion. It thus displays prominantly the spectrum of confined quarks in a very simple way.

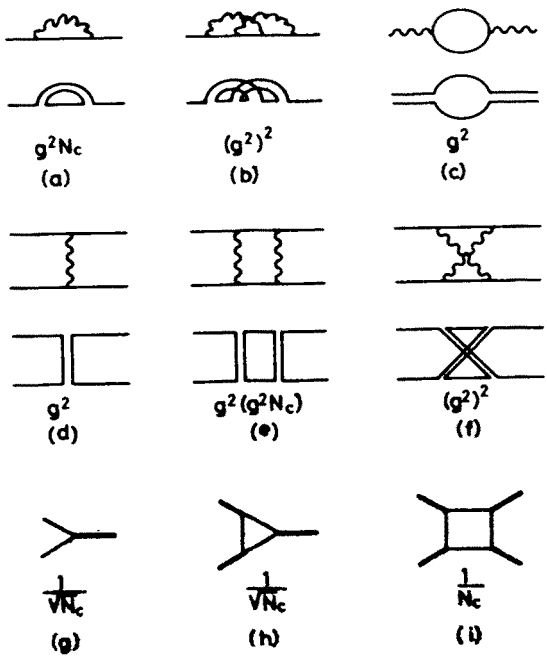

Fig. 3. Colour factors in QCD

We recall briefly the basic idea of the $1/N_c$ expansion [7]. The colour content of a quark propagator is represented by a single line which indicates the propagation of any one of the N_c colours. The colour content of a gluon propagator is represented by two lines which correspond to the propagation of one of the N_c^2 states. (Actually the colour singlet contribution should be removed leaving $N_c^2 - 1$ states. This gives higher order cor-

rections in $1/N_c$ and will not concern us here.) Some examples of Feynman graphs and corresponding colour factors are shown in Fig. 3. Note that each closed colour loop gives a factor N_c. One finds in general the leading order term in $1/N_c$ for given external lines consists of all planar graphs with no extra fermion loops. Higher order contributions have a more complicated topology of gluon lines ($1/N_c^2$ for each additional handle — see Figs. 3b and 3f) or additional fermion loops ($1/N_c$ for each loop — see Fig. 3c). Note that if there is resonance in the $q\bar{q}$ channel in leading order $1/N_c$ (lowest order graphs shown in Figs. 3d and 3e) then its coupling to $q\bar{q}$ is of order $1/\sqrt{N_c}$ (Fig. 3g). Consequently the three-meson vertex is of order $1/\sqrt{N_c}$ (Fig. 3h) and the resonance width vanishes like $1/N_c$. If the theory confines the only states in the $q\bar{q}$ channel are zero width resonances in leading order $1/N_c$. Thus if the amplitudes satisfy unsubtracted dispersion relations in leading order $1/N_c$ they give a dual resonance model. The $1/N_c$ expansion plays an important practical role in QCD_2. The leading order term can be obtained and studied relatively easily. Indeed we shall focus our attention on the leading term here. In principle higher order contributions can be constructed from it by an expansion equivalent to the dual loop expansion in dual models.

The $1/N_c$ expansion emphasizes strongly resonance physics. According to Veneziano [7], as N_c is decreased a multiperipheral picture becomes more and more appropriate. Since N_c is in fact not too large, perhaps resonance dominance is not the most appropriate picture phenomenologically. This must be borne in mind in interpreting the results of our calculations. A related problem is that the $1/N_c$ expansion, like perturbative expansions in a coupling constant, has the property that unitarity is not satisfied if the leading terms are taken for each amplitude. Thus the right-hand side of the unitarity equation $\mathrm{Im}\, A = |A|^2$ has an explicit N_c dependence which is of higher order than the left-hand side. This means, for example, that there are difficulties in interpreting phenomenologically expressions for inclusive cross-sections (see Refs. [27] and [31] below). We shall not discuss these issues further here.

2.2. The light-cone gauge

't Hooft [4] originally suggested studying QCD_2 in the light-cone gauge and since then all studies of physical processes in QCD_2 have been based on this starting point. The first advantage of the light-cone gauge, e. g.,

$$A_- = \frac{1}{\sqrt{2}}(A_0 - A_1) = 0 \tag{2.1}$$

or indeed any axial gauge, is that there are no ghosts and all triple and quadruple gluon vertices vanish since $[A_\mu, A_\nu]$ which occurs in $G_{\mu\nu}$ vanishes. Furthermore if light-cone variables, e. g.,

$$k_\pm = \frac{1}{\sqrt{2}}(k_0 \pm k_1), \tag{2.2}$$

are used in the loop integrals, the k_+ integrals can be done easily leading to simple x_- ordered perturbation theory expressions.

In the light-cone gauge (2.1) the Green's function for the gluon field satisfies

$$\partial_-^2 A_+ = \delta^2(x)$$

and thus

$$A_+(x_+, x_-) = \delta(x_-)\left[\tfrac{1}{2}|x_+| + Bx_+ + C\right]. \tag{2.3}$$

The C term reflects a further gauge freedom and can be suppressed [8] while the B term corresponds to a constant background electric field which is irrelevant for amplitudes

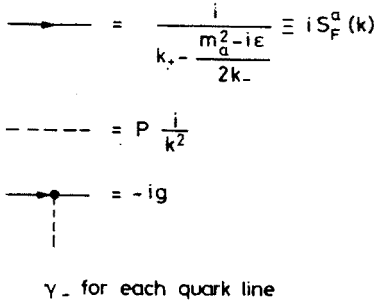

Fig. 4. Simplified Feynman rules for QCD_2. The subscript a on the quark mass m_a specifies the flavour

involving colour singlets [9]. To obtain the Fourier transform of the linearly growing potential $|x_+|$ we need to cut it off somehow at large "distances". A natural cut-off is

$$A_+ \to \delta(x_-)\,\tfrac{1}{2}|x_+|e^{-\varepsilon|x_+|} \tag{2.4}$$

which gives for the gluon propagator

$$P\frac{i}{k_-^2} = \frac{i}{2}\left(\frac{1}{(k_- + i\varepsilon)^2} + \frac{1}{(k_- - i\varepsilon)^2}\right). \tag{2.5}$$

Note that the ε here has nothing to do with specifying the boundary conditions for incoming or outgoing waves but is instead required by the strong long-distance singularity in (2.3).

In two dimensions, the gamma-matrix algebra is very simple and one arrives at the simplified Feynman rules shown in Fig. 4. To avoid confusion with the photon and emphasize the potential nature of the gluon from now on we indicate it by a dotted line.

2.3. Bound states

We start our study of QCD_2 by investigating the bound states in the $q\bar{q}$ channel. We consider the $q\bar{q}$ T matrix which consists of graphs of the form of Figs 3d and 3e with quark self-mass insertions (Fig. 3a). The self-mass contributions are easily taken care of. Only the graph of Fig. 3a and its iterations give non-vanishing contributions and these lead simply to a renormalization of the quark mass

$$m_a^2 \to \tilde{m}_a^2 = m_a^2 - m^2, \tag{2.6}$$

where

$$m^2 = g^2 N_c/\pi. \tag{2.7}$$

The T matrix thus satisfies the integral equation shown in Fig. 5

$$iT(q, q'; p) = \frac{-ig^2}{(q_- - q'_-)^2} - g^2 N_c \int \frac{d^2k}{(2\pi)^2} \frac{S_F^a(k) S_F^b(k-p)}{(k_- - q_-)^2} T(k, q'; p), \tag{2.8}$$

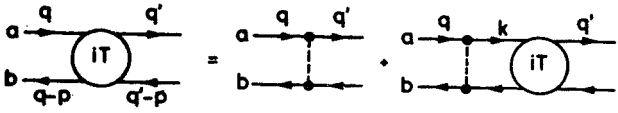

Fig. 5. Equation for $q\bar{q}$ T matrix

where T is the coefficient of γ_- for each of the upper and lower quark lines. If there is a bound state at $p^2 = m_n^2$, then the meson $q\bar{q}$ vertex satisfies the equation shown in Fig. 6

$$\Gamma_n^{a\bar{b}}(q; p) = \frac{ig^2 N_c}{(2\pi)^2} \int \frac{d^2k}{(k_- - q_-)^2} S_F^a(k) S_F^b(k-p) \Gamma_n^{a\bar{b}}(k; p). \tag{2.9}$$

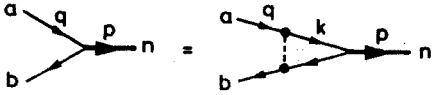

Fig. 6. Equation for $\Gamma_n(q', p)$

We define equal "time" ($x_- = 0$) wave function

$$\phi_n^{a\bar{b}}(x) \equiv \frac{i}{4\pi} \int_{-\infty}^{\infty} dq_+ e^{ix-q+} S_F^a(q) S_F^b(q-p) \Gamma_n^{a\bar{b}}(q; p)|_{x_- = 0}, \tag{2.10}$$

where $x \equiv q_-/p_-$. Performing the integral yields

$$\phi_n^{a\bar{b}}(x) = -\frac{1}{m_n^2 - \dfrac{\tilde{m}_a^2}{x} - \dfrac{\tilde{m}_b^2}{1-x}} \Gamma_n^{a\bar{b}}(x), \tag{2.11}$$

where

$$\Gamma_n^{a\bar{b}}(q; p) \equiv \frac{1}{p_-} \Gamma_n^{a\bar{b}}(x).$$

Substituting (2.11) into (2.9) gives 't Hooft's equation [4] for the bound states

$$H\phi_n^{a\bar{b}}(x) = m_n^2 \phi_n^{a\bar{b}}(x), \tag{2.12}$$

where

$$H = H_0^{ab} + V, \tag{2.13}$$

and

$$H_0^{ab} = \frac{\tilde{m}_a^2}{x} + \frac{\tilde{m}_b^2}{1-x}, \qquad V = -m^2 P \int_0^1 \frac{dy}{(x-y)^2}. \tag{2.14}$$

If Eq. (2.12) is divided by $2p_-$ it is recognizable as an equation for the total "energy" p_+ of the bound state (p_+ is conjugate to the "time" x_-). H_0 gives the on-mass-shell value of the kinetic energy of the quarks

$$\frac{1}{2p_-}\frac{\tilde{m}_a^2}{x} = \frac{1}{2p_-}\frac{2q_-q_+}{q_-/p_-} = q_+$$

and V is just the Fourier transform of the potential energy $m^2|x_+|$ due to gluon exchange. Generally, performing loop integrals over (+) components leads to expressions like those of old-fashioned perturbation theory where the denominators are differences of (+) components of momenta of on-mass-shell particles. For example, the equation corresponding to Fig. 6 can be written down by inspection:

$$\Gamma_n = V \frac{1}{m_n^2 - H_0}\Gamma_n \tag{2.15}$$

which is equivalent to (2.12). Note that the action of H is only defined on functions which vanish at $x = 0$ and $x = 1$ so we must restrict our consideration to such functions.

It has been demonstrated that the discrete spectrum of the 't Hooft equation extends to arbitrarily high masses and forms a complete set of states [10]. There are therefore no $q\bar{q}$ thresholds in the $q\bar{q}$ channel and hence the quarks are confined as we expected.

In our study of high-energy processes we will need some properties of the wave functions ϕ_n for large m_n^2. A WKB approximation for ϕ_n for large n is suggested by thinking of the momentum fraction $x\,[= q_-(1/p_-)]$ as a co-ordinate. The conjugate variable is the separation between the quarks which we call $p\,[= (x_{a+} - x_{b+})(p_-)]$. The classical Hamiltonian corresponding to Eq. (2.13) is then [11, 12]

$$\frac{1}{\pi m^2} H_{cl} = |p| + U(x), \tag{2.16}$$

where

$$U(x) = \frac{1}{\pi}\left[\frac{\tilde{m}_a^2/m^2}{x} + \frac{\tilde{m}_b^2/m^2}{1-x}\right].$$

This looks like a photon moving in a potential $U(x)$. The standard WKB procedure is to calculate the action using the classical orbits

$$S(x) = \int^x |p| dx = \int^x [E - U(x)]dx, \tag{2.17}$$

where $E = 2p_+p_-/\pi m^2$ and obtain the WKB wave function

$$\phi(x) = Ae^{\pm iS(x)}. \tag{2.18}$$

The quantization condition is

$$\oint |p| dx = 2\pi n + B, \tag{2.19}$$

where B is related to the phase shift at the classical turning points.

The difficult part of the problem is the analysis of the behaviour near the turning points. For $\phi_n(x) \sim \exp(\pm in\pi x)$ which follows from (2.18) and (2.19) one sees that $U \approx |p|$ at $x \approx 1/n$ and $1-x \approx 1/n$. Thus for large n the turning points are very near the singularities of the potential U. This makes the full solution particularly difficult. However, by evaluating

$$m_n^2 = \int_0^1 \phi_n(x)\,[H\phi_n(x)]dx$$

using $\phi_n(x) \propto e^{\pm inx}$ we see that

$$(m_n^{a\bar{b}})^2 \sim \pi^2 m^2 n + (\tilde{m}_a^2 + \tilde{m}_b^2) \ln n + C^{a\bar{b}}, \tag{2.20}$$

where the term proportional to n arises from V and the term proportional to $\ln n$ from H_0. Hence we have

$$\phi_n^{a\bar{b}}(x) = A \exp\left[\pm \frac{i}{\pi m^2} \int^x [m_n^2 - H_0^{a\bar{b}}(x')]dx'\right] \tag{2.21}$$

which determines ϕ_n to within a constant phase.

To determine the constants in Eqs. (2.20) and (2.21) we need to study the regions $x \approx 1/n$ and $1-x \approx 1/n$. If we write

$$x \equiv \frac{m^2}{m_n^2}\,\xi \tag{2.22}$$

then for finite ξ, $x \approx 1/n$ and 't Hooft's equation goes over into the scaling form [8]:

$$\phi^a(\xi) = \frac{\tilde{m}_a^2}{m^2}\,\frac{1}{\xi}\,\phi^a(\xi) - P\int_0^\infty d\eta\,\frac{\phi^a(\eta)}{(\eta-\xi)^2}, \tag{2.23}$$

where

$$\phi^a(\xi) \equiv \lim_{n\to\infty} \phi_n^{a\bar{b}}\left(\frac{m^2}{m_n^2}\,\xi\right).$$

If we require that (2.21) goes over into a scaling form $\phi^a(\xi)$ for $x \approx 1/n$ and $\phi^b(\xi)$ for $1-x \approx 1/n$ we find to $O(1/n)$ [11, 13]

$$(m_n^{a\bar{b}})^2 \sim \pi^2 m^2 n + (\tilde{m}_a^2 + \tilde{m}_b^2) \ln n + C(\tilde{m}_a^2) + C(\tilde{m}_b^2),$$

$$\phi_n^{a\bar{b}}(x) \sim \sqrt{2} \sin\left[n\pi x + \delta_n^{a\bar{b}}(x)\right],$$

$$\phi^a(\xi) \sim \sqrt{2} \sin\left[\frac{1}{\pi}\,\xi + \delta^a(\xi)\right] \quad (\xi \text{ large}), \tag{2.24}$$

where

$$\pi\delta_n^{a\bar{b}}(x) = -\tilde{m}_a^2(\ln xn - x\ln n) + \tilde{m}_b^2(\ln(1-x)n - (1-x)\ln n) - C(\tilde{m}_a^2)(1-x) + C(\tilde{m}_b^2)x \tag{2.25}$$

and

$$\pi\delta^a(\xi) = -\frac{\tilde{m}_a^2}{m^2}\ln\frac{\xi}{\pi^2} - C(\tilde{m}_a^2).$$

Furthermore a detailed study [11] of (2.23) gives as explicit expression for $C(\tilde{m}^2)$ and the following result which we will see plays a crucial role below:

$$\int_0^\infty \frac{d\xi}{\xi}\phi^a(\xi) = \left(\frac{\tilde{m}_a^2}{m^2}+1\right)^{-1}\int_0^\infty d\xi\phi^a(\xi) = \frac{\pi}{\sqrt{\frac{\tilde{m}_a^2}{m^2}+1}}. \tag{2.26}$$

Finally we note that the behaviour of ϕ at $x = 0,1$ is easily obtained by trying a power behaviour [4]

$$\phi_n^{a\bar{b}}(x) \sim C_n^{a\bar{b}}x^{\beta_a} \quad (x \to 0) \tag{2.27}$$

and one finds

$$\pi\beta_a \cot\pi\beta_a = -\frac{m_a^2}{m^2}. \tag{2.28}$$

Note $\beta_a \to 0$ as $m_a \to 0$ and $\beta_a \to 1$ as $m_a \to \infty$. The wave functions have the "parity" property

$$\phi_n^{a\bar{b}}(x) = (-1)^n\phi_n^{b\bar{a}}(1-x). \tag{2.29}$$

2.4. Some general properties of light-cone gauge amplitudes

Amplitudes calculated in the light-cone gauge according to the prescription of Section 2.2 are functions of the invariants and ratios of the $(-)$ momentum components (i.e., x variables). Hence they are manifestly invariant under proper Lorentz transformations (actually there is only one transformation, a boost in the 1 direction). Parity invariance is not obvious, however. No non-trivial check of parity invariance has yet been made. Parity invariance is clearly equivalent to gauge invariance under the change of gauge $A_- = 0 \to A_+ = 0$. We shall return to the question of gauge invariance in the Appendix.

As is often the case when one uses a non-covariant gauge, individual Feynman graphs have singularities which are not present in the sum of all graphs contributing to a physical (gauge invariant) amplitude. This can be simply illustrated by considering the quark form factor in order g^2 (Fig. 7) [14]. We have

$$i\Gamma_-^{(2)} = i\gamma_- N_c\int\frac{d^2k'}{(2\pi)^2}(-ig)^2\frac{i}{k'_+ - \frac{m_a^2-i\varepsilon}{2k'_-}}\quad\frac{i}{(k'_+-q_+)-\frac{m_b^2-i\varepsilon}{2(k'_--q_-)}}\left(\frac{i}{(k_--k'_-)^2}\right),$$

where we have restricted ourselves to the $(--)$ component for simplicity. The quark masses are the bare masses, self-energy insertions simply take the bare masses to the renormalized masses in the lowest order graph (which is actually independent of m_i^2).

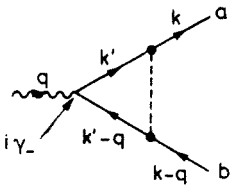

Fig. 7. Quark form factor in order g^2

As usual the k'_+ integral is performed easily giving ($x \equiv k_-/q_-$)

$$\Gamma_-^{(2)} = \gamma_- \Gamma^{(2)}(q^2, x),$$

where

$$\Gamma^{(2)}(q^2, x) = V \frac{1}{q^2 - H_0(x)} = -m^2 P \int_0^1 dx' \frac{1}{(x-x')^2} \frac{1}{q^2 - \dfrac{m_a^2}{x} - \dfrac{m_b^2}{1-x}}$$

$$\equiv \frac{m^2}{q^2} \frac{d}{dx} I(q^2, x) \tag{2.30}$$

with

$$I(q^2, x) = P \int_0^1 dx' \frac{1}{x'-x} \frac{x'(1-x')}{(x'-r_+)(x'-r_-)}. \tag{2.31}$$

The roots

$$r_\pm = \tfrac{1}{2}\left[1 + \frac{m_a^2}{q^2} - \frac{m_b^2}{q^2} \pm \sqrt{\lambda\left(1, \frac{m_a^2}{q^2}, \frac{m_b^2}{q^2}\right)}\right] \tag{2.32}$$

are the two ($k_z \lesseqgtr 0$) on-mass shell values of x. The integral in (2.31) is straightforward to perform

$$I(q^2, x) = \frac{x(1-x)}{(x-r_+)(x-r_-)} \ln\left|\frac{1-x}{x}\right| - \frac{r_+(1-r_+)}{(x-r_+)(r_+-r_-)} \ln\frac{1-r_+}{-r_+}$$

$$- \frac{r_-(1-r_-)}{(x-r_-)(r_--r_+)} \ln\frac{1-r_-}{-r_-}. \tag{2.33}$$

For $q^2 < 0$, r_+ and r_- are not in [0,1] and the arguments of the final two logarithms are positive. For $q^2 > (m_a+m_b)^2 + i\varepsilon$, the arguments are negative and

$$\ln[(1-r_\pm)/-r_\pm] \to \ln[(1-r_\pm)/r_\pm] \mp i\pi.$$

The mass shell singularities at $x = r_\pm$ are present in Eq. (2.33) (and thus also Eq. (2.30)) only for $q^2 > (m_a + m_b)^2$ where the physical production of a $q\bar{q}$ pair can take place. The apparent singularities in the real part of (2.33) cancel as expected since the singularity arises from a pinch of the singularities in Eq. (2.31) at $x' = x$ and $x' = r_\pm$ which can only take place for x and $r_\pm$ in [0,1]. The mass shell singularities are double poles in Γ in order g^2. When all orders are summed the infinities conspire to give a vanishing of Γ on the mass shell [8]. They are therefore perturbative manifestations of confinement. Note, however, that Γ does not vanish (or, in perturbation theory, blow up) on the mass shell for $q^2 < 0$ ($x = r_+ > 1$ or $x = r_- < 0$) corresponding to the process quark + current → quark. This means that if we are in a sector containing a quark, nothing prevents it from interacting. To avoid the production of quarks in physical processes involving only colour singlets we need the vanishing of Γ on-shell only for q^2 above threshold. Although this requirement is weaker than the vanishing on-mass-shell for all q^2 which is the confinement signal often discussed, it is sufficient to assure confinement in physical processes.

The singularities at $x = 0,1$ in Eq. (2.33) are new features of QCD_2. They have important (and peculiar) consequences. The logarithmic divergence of $\Gamma^{(2)}$ as $x \to 0$ (or $x \to 1$),

$$\Gamma^{(2)} \underset{x\to 0}{\sim} -\frac{m^2}{m_a^2} \ln |x|, \tag{2.34}$$

is a perturbative manifestation of the behaviour (2.27) of the wave function $\phi(x)$. We note that $\phi(x)$ is analogous to

$$-\frac{1}{q^2 - H_0(x)}\Gamma(x),$$

(see Eq. (2.11)) and hence

$$\phi(x) \to -\frac{\Gamma(x)}{q^2 - H_0(x)} \sim x(\Gamma^{(0)} + \Gamma^{(2)} + \cdots) \sim x\left(1 - \frac{m^2}{m_a^2} \ln x + \cdots\right) \tag{2.35}$$

which agrees with (2.27) since $m^2 \to 0$ as $g^2 \to 0$ and thus

$$\beta \to 1 - \frac{m^2}{m_a^2} \approx 1 - \frac{m^2}{m_a^2}.$$

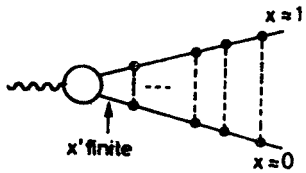

Fig. 8. Development of "wee" partons through many iterations of the confining potential

The behaviour $\phi(x) \sim x$ is the usual behaviour given by the "spectator rule" [15] for a hadron composed of two constituents in non-confining models. We see that in QCD_2 the probability of finding a "wee" parton in a hadron is *enhanced* compared to the usual behaviour in a superrenormalizable theory due to the singular nature of the confining

potential. "Wee" partons can be produced through many soft exchanges (see Fig. 8). This enhanced probability is responsible for Regge behaviour in QCD_2, asymptotie behaviour of form factors differing from the dimensional counting results [15] and somc important features of e^+e^- annihilation cross-section ($\gamma^* \to hX$). These consequences will be explored below. We now turn to an apparently "peculiar" consequence of these singularities.

Since the singularities at $x = 0,1$ arise from the collision of the singularities of $P(1/(x-x')^2)$ with the end-points of integration they lead to the non-analytic behaviour in x of $\ln|(1-x)/x|$. Thus the amplitudes for x in [0,1] and x outside [0,1] are *not* related by analytic continuation. For $k^2 > 0$ and $(q-k)^2 > 0$, x in [0,1] corresponds to the process (current $\to q_a\bar{q}_b$) while $x > 1$ corresponds to (q_b + current $\to q_a$) and $x < 0$ to $\bar{q}_a$ + current $\to \bar{q}_b$). Thus the first of these processes is not related to the other two by (analytic continuation due to the singularities at $x = 0,1$ arising from the confining potential (2.4). Such behaviour is not without precedent in models of confinement [16].

The quark form factor for off-mass-shell quarks is not a gauge invariant amplitude. If we consider a gauge invariant amplitude we may hope to find better analytic properties. On-mass-shell quark amplitudes would seem to be likely candidates. However, we have seen that these do not generally exist in a confining theory. Amplitudes involving colourless (but perhaps flavourful) currents are physical and thus might be expected to have normal analyticity properties. However, because of confinement, singularities are worse than those normally encountered, so analyticity should be checked carefully! (Amplitudes with external mesons can be obtained by extracting the residues of the poles at m_π^2.)

For example, the three-current amplitude in order g^2 is the sum of the three Feynman graphs shown in Fig. 9. For each individual graph the processes with $q_i^2 < 0$ and q_i^2 above threshold are not related by analytic continuation due to the behaviour of the quark form

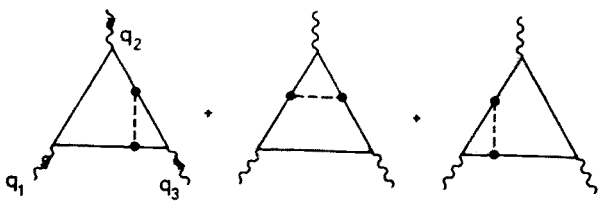

Fig. 9. Three-current amplitude in order g^2

factor discussed above. However, for the sum of all three graphs these processes are indeed related by analytic continuation [14] as is normally expected. It should be emphasized that if not all three currents are colour singlets, the graphs in Fig. 9 occur with different weights and normal analyticity is lost.

These results can be generalized to the sum of all graphs in leading order $1/N_c$. We have explicitly verified [14] that the three-current and four-current amplitudes for crossed processes are related by analytic continuation. Meson amplitudes therefore have the same property. Furthermore, assuming parity invariance, we have shown that the only singulari-

ties are poles due to the bound states of Eq. (2.12). The amplitudes thus have the properties expected in leading order $1/N_c$ [7].

We therefore believe that physical colour-singlet amplitudes in QCD_2 have all the usual properties required of scattering amplitudes and thus QCD_2 is an acceptable model for hadrons.

2.5. "Soft" hadronic processes in QCD_2

We conclude this section by recalling some of the features of purely hadronic processes in QCD_2 [17, 18]. The meson-meson scattering amplitude has a behaviour at high energies characteristic of Regge pole exchange in four dimensions. The amplitude for the process shown in Fig. 10 has the behaviour as $s \to \infty$

$$A^{st} \sim R_{11'}R_{22'}(-s)^{-\beta_a-\beta_d}. \tag{2.36}$$

Note that the power of s is non-integral and depends only on the exchanged quarks (a, $\bar{d}$). Furthermore the coefficient factorizes into a part depending on the upper two mesons and a part depending on the lower two mesons. These features are reminiscent of a factorizable

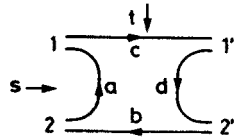

Fig. 10. Quark line diagram for meson-meson scattering

Regge exchange in the t channel. Since we are restricted to forward scattering in two--dimensions, we cannot look for the characteristic t dependence of the power of s. Equation (2.34b) thus does not represent true Regge behaviour but only an "embryonic" Regge behaviour with

$$\alpha_{a\bar{d}}(0) \equiv -\beta_a-\beta_d. \tag{2.37}$$

The Regge behaviour (2.36) has the parton model interpretation of reflecting the exchange of "wee" partons advocated by Feynman [1]. Suppose we are in the centre-of--mass frame with meson 1 moving to the left so $\sqrt{2}p_{1-} \sim \sqrt{s}$ and $\sqrt{2}p_{2-} \sim m_2^2/\sqrt{s}$. Then

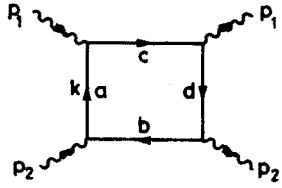

Fig. 11. Perturbation theory analogue to meson-meson scattering

the decreasing power behaviour $s^{-\beta_a}$ in (2.36) can be seen to arise from the small amplitude ($\approx x^{\beta_a}$) for finding a "wee" quark in the "fast" meson 1 which can annihilate one of the necessarily slow quarks in meson 2 (i.e., $k_{a-} \approx p_{2-} \approx (m_2^2/s)p_{1-}$ yielding $x \equiv k_{a-}/p_{1-} \sim m_2^2/s$).

This parton interpretation of (2.36) can be illustrated simply in perturbation theory. As analogues of the external mesons we consider the (−) components of vector currents

[19]. The analogue of Fig. 10 in lowest order perturbation theory is then the simple box graph shown in Fig. 11. Using the Feynman rules of Fig. 4, we easily obtain

$$\operatorname{disc}_s A_{--} = iN_c \int \frac{d^2k}{(2\pi)^2} \frac{1}{k_+ - \dfrac{m_a^2}{2k_-}} \frac{1}{k_+ - \dfrac{m_d^2}{2k_-}} \left[-2\pi i\delta\left(k_+ + p_{1+} - \frac{m_c^2}{2(k+p_1)_-}\right)\right]$$

$$\times \left[-2\pi i\delta\left(k_+ - p_{2+} - \frac{m_b^2}{2(k-p_2)_-}\right)\right] \tag{2.38}$$

$$\approx i4N_c(p_{1-})^2(p_{2-})^2 \int dx \frac{1}{p_1^2 - H_0^{ac}(x)} \frac{1}{p_1^2 - H_0^{dc}(x)} \delta\left(s - \frac{m_b^2}{x} - \frac{m_c^2}{1-x}\right), \tag{2.39}$$

where x is defined as above. The two factors in brackets can be interpreted as the wave functions of the initial and final meson 1 in zeroth order perturbation theory (see Eq. (2.35)). Since the δ function requires $x \approx m_b^2/s$ (or $1-x \approx m_c^2/s$) we see the amplitude has the behaviour s^{-2} which arises from the small probability for finding a slow quark in the fast meson:

$$\operatorname{Im} A \approx [\phi(x)]^2|_{x\sim\frac{1}{s}} \sim \frac{1}{s^2}.$$

In higher orders of perturbation theory the wave function is modified as in Eq. (2.35) and the amplitude is larger ($A \sim s^{-\beta_a-\beta_a}$) due to the enhanced probability of finding a "wee" quark discussed in Section 2.4.

As we have emphasized above the mechanism for producing "wee" quarks in QCD_2 seems to be particular to confinement. "Wee" partons arise through many iterations of the confining potential and not through the usual multiperipheral mechanism which involves the gradual degradation of parton momentum through successive virtual decays [20]. Therefore in a confining theory the origin of Regge exchange may be quite different from in conventional non-confining theories from which multiperipheral models arose [21].

It is quite amusing that, even for "soft" hadronic processes where short-distance arguments are inapplicable, QCD_2 has a simple parton model interpretation. The above discussion can in fact be generalized to multi-particle processes. Factorizable multi-"Regge" behaviour obtains [17, 22] and can be interpreted in terms of a generalization of Feynman's parton picture.

3. The parton model and two-dimensional QCD

3.1. The parton model and short-distance processes

We begin by discussing how the parton model results for light-cone dominated processes are realized in the physical region, i.e., how it is that the quarks behave "as if" they are free even though they are confined in meson bound states. We start with the simplest process: the e^+e^- annihilation total cross-section [8, 11, 23].

For $q^2 \to -\infty$, the deep Euclidean region, we can be certain that the lowest order graph (Fig. 12) dominates since QCD_2 is super-renormalizable and higher order graphs therefore behave like $(g^2/q^2)^n$. For clarity we have allowed the two quarks to have different flavours a and b since the same analysis applies to a flavour changing current. Considering the $(-)$ component of a vector current for simplicity we have

$$A_{--} = -q_- q_- \frac{e_{ab}^2 N_c}{\pi} \int_0^1 dx \frac{1}{q^2 - \frac{m_a^2}{x} - \frac{m_b^2}{1-x}}, \tag{3.1}$$

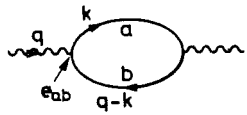

Fig. 12. Dominant graph for e^+e^- annihilation total cross-section as $q^2 \to -\infty$

where $x = k_-/q_-$. Using the analogue of (2.32) we have

$$A_{--} = \frac{q_- q_-}{q^2} \frac{e_{ab}^2 N_c}{\pi} \int_0^1 dx \frac{x(1-x)}{(x-r_+)(x-r_-)}$$

$$\underset{q^2 \to -\infty}{\sim} -\frac{q_- q_-}{q^2} \frac{e_{ab}^2 N_c}{\pi} \left[1 + \frac{m_a^2 + m_b^2}{q^2} \ln(-q^2) + \cdots\right]. \tag{3.2}$$

Note that it is, of course, the unrenormalized quark mass which occurs in all the above expressions.

What we are really interested in is the imaginary part of A_{--} for $q^2 \to +\infty$. Equation (3.2) appears to have such an imaginary part if we naively continue it to $q^2 \to +\infty$

$$\text{Im } A_{--} \sim q_- q_- e_{ab}^2 N_c \frac{m_a^2 + m_b^2}{q^4}. \tag{3.3}$$

However, this corresponds to the propagation of free quarks:

$$x = r_- \sim \frac{m_a^2}{q^2} \quad \text{or} \quad x = r_+ \sim 1 - \frac{m_b^2}{q^2} \tag{3.4}$$

and certainly is not strictly correct since the quarks are confined. How can we then obtain information on the physical region from (3.2)?

We expect (3.2) to be a good approximation as long as we stay away from the positive $-q^2$ axis where non-perturbative confinement effects are important and give rise to bound states. Thus (3.2) should hold along rays in the complex $-q^2$ plane. Consideration of a ray at a small angle to the positive axis suggests that (3.2) should represent the behaviour in the physical region in some average sense [24, 25]. To make this precise [25] consider

the contour C in the complex $-q^2$ plane shown in Fig. 13. Along the large circles we expect (3.2) to be a good approximation. Applying Cauchy's theorem to $\tilde{A} \equiv (q^2/q_-q_-)A_{--}$ we have

$$0 = \int_0^{2\pi} Q_2^2 e^{i\theta} i d\theta \tilde{A} - \int_0^{2\pi} Q_1^2 e^{i\theta} i d\theta \tilde{A} - 2\pi i \sum_{n=n_1}^{n_2} \mathrm{Res}_{q^2=m_n^2} \tilde{A}, \tag{3.5}$$

where the sum arises from the parts of the contour near the real axis. Carrying out the integrals gives

$$-\frac{1}{\pi m^2} \frac{1}{(n_2 - n_1 + 1)} \sum_{n=n_1}^{n_2} \mathrm{Res}_{q^2=m_n^2} A \sim \frac{q_-q_-}{q^4} e_{ab}^2 N_c (m_a^2 + m_b^2) \tag{3.6}$$

for $Q_2^2 \gtrsim Q_1^2 \gg m^2$, which simply states that the parton model result gives the average over the actual bound state poles [26].

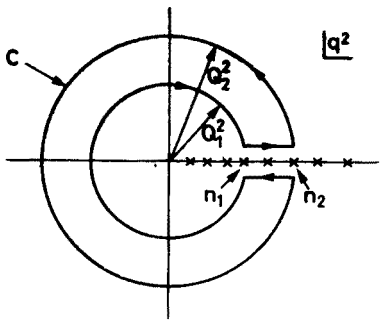

Fig. 13. Contour used in Eq. (3.5)

The above result is based only on general principles (deep Euclidean behaviour and analyticity) so it should hold in QCD_2. Let us see how this happens. Each bound state in q^2 at $q^2 = m_n^2$ gives a delta-function contribution to Im A_{--}. If we average such a contribution over the spacing $\pi^2 m^2$ between bound states we have [8]

$$\mathrm{Im}\, A_{--} \equiv q_-q_- \frac{1}{\pi m^2} (g_n^V)^2 = q_-q_- \frac{e_{ab}^2 N_c}{\pi^2 m^2} \left[\int_0^1 dx \phi_n^{a\bar{b}}(x) \right]^2. \tag{3.7}$$

To verify (3.6) we need to calculate the integral of the wave function. For large n, ϕ_n oscillates rapidly (Eq. (2.24)) (see Fig. 14) leading to a cancellation between the positive and negative excursions. Only near the end-points will there be an imperfect cancellation. So we can write (Eqs. (2.22), (2.23) and (2.29))

$$\int_0^1 dx \phi_n^{a\bar{b}}(x) \underset{n\to\infty}{\sim} \frac{m^2}{m_n^2} \left[\int_0^\infty d\xi \phi^a(\xi) + (-1)^n \int_0^\infty d\xi \phi^b(\xi) \right].$$

Then from Eq. (2.26) we have

$$\int_0^1 dx \phi_n^{a\bar{b}}(x) \underset{n\to\infty}{\sim} \frac{1}{\pi n}\left[\frac{m_a}{m} + (-1)^n \frac{m_b}{m}\right]. \tag{3.8}$$

Substituting (3.8) into (3.7) and neglecting the cross terms proportional to $(-1)^n$ which average to zero verifies Eq. (3.6).

We have therefore verified [11] that the e^+e^- annihilation cross-section which is given exactly by Eq. (3.7) can be computed on the average using the parton model as if the

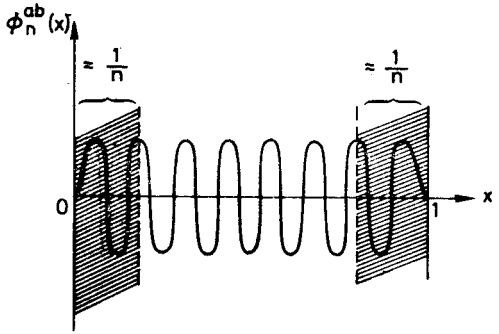

Fig. 14. $\phi_n^{a\bar{b}}(x)$ for large n. The shaded region dominates in Eq. (3.8)

quarks were free, i.e., Eq. (3.3). It is amusing to note [8] that the rapid oscillation of the bound state wave functions means the important values of the quark momenta are $x \approx 1/m_n^2$ and $1-x \approx 1/m_n^2$ which are near the mass-shell values (3.4). This is the assumption usually made in the naive parton model.

We now turn to deep inelastic scattering [8, 11]. According to light-cone dominance we expect the cross-section to be given by the imaginary part of the parton model "handbag"

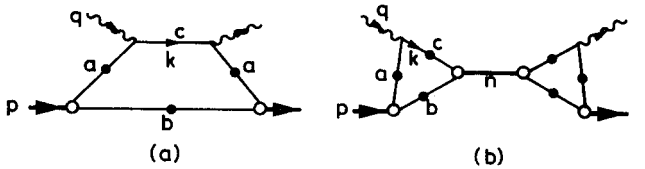

Fig. 15. Deep inelastic scattering: (a) "handbag" graph; (b) actual dominant graph

diagram shown in Fig. 15a. (There will be another term where the current strikes quark b but this is treated identically.) Quarks a and b have their renormalized propagators, explicitly indicated here, but c does not.

We will first see how the "handbag" result arises in perturbation theory [27]. As we have seen in Section 2.4, the qualitative features of confinement already manifest themselves in $O(g^2)$ since a single gluon exchange already gives a long-range force. We consider deep inelastic scattering off the $(-)$ component of a vector current [19] of mass p^2. To zeroth order in g^2 the amplitude is the same as that studied in Section 2.5 (Fig. 11 and Eq.

(2.38)). The Bjorken scaling limit can be obtained by taking $q_+ \to \infty$ while holding fixed [8]

$$x_B \equiv -q_-/p_-. \tag{3.9}$$

Using the standard Breit frame (see Eq. (3.33) below), for example, it is easy to see this is identical to the conventional $x_B = -q^2/2p \cdot q$ in the scaling limit. The mass-shell constraints now give

$$k_- \approx -q_- + \frac{m_c^2}{s}(p_- + q_-)$$

and thus [19]

$$\text{Im } A^{(0)}_{--} \sim (p_- + q_-)^2 \frac{4\pi m_c^2 e_{ac}^2}{s^2} \left[\frac{1}{p^2 - \dfrac{m_a^2}{x_B} - \dfrac{m_b^2}{1-x_B}} \right]^2, \tag{3.10}$$

where $s = (p+q)^2$. The factor in brackets is just the square of the wave function (2.35) in lowest order. ($\Gamma = 1$) and so (3.10) is the QCD_2 version of the conventional Bjorken scaling deep inelastic cross-section [28].

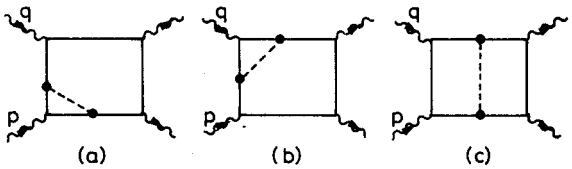

Fig. 16. Model deep inelastic amplitude in $O(g^2)$

In order g^2 there are quark self-energy contributions which take $m_i^2 \to \tilde{m}_i^2$ in Eq. (3.10) and in addition the graphs of Fig. 16 (plus analogous graphs with gluon exchanges on the right). The graph of Fig. 16a has the form

$$A^{(2a)} = A^{(0)} \Gamma^{(2)}_{ab}(p^2, x_B), \tag{3.11}$$

where $\Gamma^{(2)}$ is given by (2.30). Similarly we have

$$A^{(2b)} = A^{(0)} \Gamma^{(2)}_{ac}(q^2, x),$$

where

$$x = -k_-/q_- \sim 1 - \frac{m_c^2}{q^2}.$$

Changing variables in (2.30) to $x' = 1 + \lambda(m_c^2/q^2)$ gives

$$\Gamma^{(2)}_{ac}(q^2, x) \sim \frac{m^2}{m_c^2} \int_0^\infty d\lambda \frac{\lambda}{(\lambda+1)^3}$$

and hence

$$A^{(2b)} \sim A^{(0)}\left(-\tfrac{1}{2}\frac{m^2}{m_c^2}\right). \tag{3.12}$$

The calculation of Fig. 16c is a little more lengthy. There are two x_- "time" orderings in this case. We summarize the results in Fig. 17, indicating denominators $(p^2-H_0)^{-1}$ by dotted lines. The graph $A^{(2c_2)}$ plus a similar graph with the discontinuity to the left has the effect of cancelling the mass renormalization of (3.10) which would be caused by the quark self-energy insertions. This same mechanism operates in the e^+e^- annihilation case studied above to remove all $O(g^2)$ effects. Graphs $A^{(2b)}$ and $A^{(2c_1)}$ cancel each other.

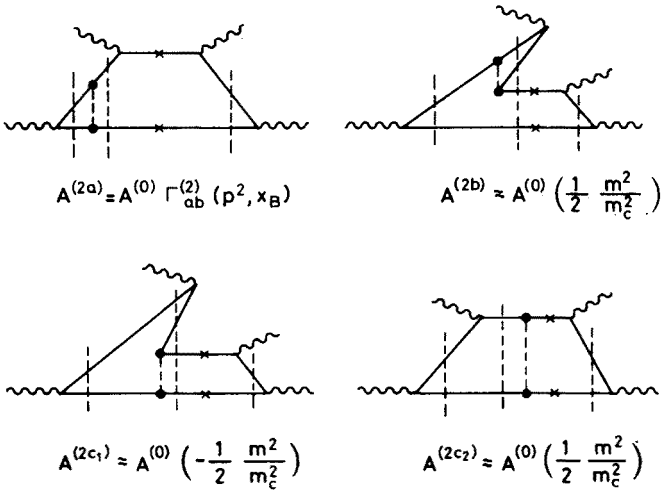

Fig. 17. "Time" ordered contributions to deep inelastic scattering in $O(g^2)$

This is an example of a very general phenomenon occurring in the model. These graphs contain the exchange of a "soft" gluon ($l_- \approx ((m^2/q^2)p_-$) from a given line to each of the two lines of the initial colour singlet state. These contributions are proportional to the colour charge and thus cancel [29]. Thus as expected the only contribution remaining is $A^{(2a)}$ which creates the wave function in $O(g^2)$ (see Eq. (2.35)):

$$\phi^{a\bar{b}}(x_B) \approx -\frac{1}{p^2-H_0^{ab}(x_B)}[1+\Gamma_{ab}^{(2)}(p^2, x_B)]. \tag{3.13}$$

It should be noted that this is not the only scaling contribution in $O(g^2)$, all the contributions in Fig. 17 scale, but the other contributions cancel. The cancellations discussed above have their counter part in the non-perturbative calculation to which we now turn.

The "handbag" graph of Fig. 15a for $(-)$ components of vector currents is given by

$$A_{--} = -4(p_-+q_-)^2 e_{ac}^2 \int_0^1 dx[\phi_h^{a\bar{b}}(x+(1-x)x_B)]^2 \frac{1}{s-\dfrac{m_c^2}{x}-\dfrac{\tilde{m}_b^2}{1-x}}, \tag{3.14}$$

where $x = k_-/p_-$. In the imaginary part only the root $x = r_- \approx (m_c^2/s)$ is important as $\phi_h^{a\bar{b}}(r_+) \approx 0$ by (2.27). We have then

$$\text{Im } A_{--} = (p_- + q_-)^2 \frac{4\pi m_c^2 e_{ac}^2}{s^2} [\phi_h^{a\bar{b}}(x_B)]^2. \tag{3.15}$$

Again, of course, in the physical region we must take into account the existence of bound states (Fig. 15b). Equation (3.15) can only be true on the average. The actual amplitude is expressible in terms of the overlap between the wave functions $\phi_h^{a\bar{b}}$ and $\phi_n^{c\bar{b}}$ [30]. Averaging the bound state contributions as usual we have

$$\text{Im } A_{--} = (p_- + q_-)^2 \frac{4e_{ac}^2}{\pi m^2} \left[\int_0^1 dx \phi_h^{a\bar{b}}(x + (1-x)x_B) \phi_n^{a\bar{c}}(x) \right]^2. \tag{3.16}$$

Again due to the rapid oscillation of ϕ_n (see Fig. 18) only the region near $x = 0$ is important. Changing to the scaling variable ξ and again using Eq. (2.26) verifies the equivalence of (3.16) and (3.15) on the average.

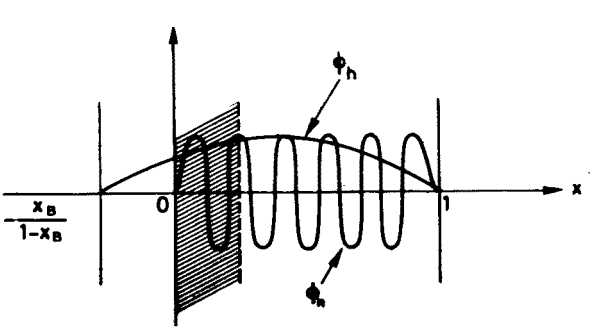

Fig. 18. Pictorial representation of integral in Eq. (3.16)

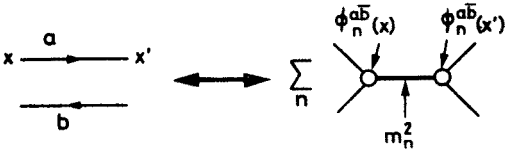

Fig. 19. Pictorial representation of Eq. (3.17)

We have seen that for these light-cone dominated processes the final state $q\bar{q}$ pair can be treated as if they were free. This can be represented graphically in Fig. 19 or

$$\frac{\delta(x-x')}{s - \frac{m_a^2}{x} - \frac{m_b^2}{1-x} + i\varepsilon} \leftrightarrow \sum_n \frac{\phi_n^{a\bar{b}}(x)\phi_n^{a\bar{b}}(x')}{s - m_n^2 + i\varepsilon}. \tag{3.17}$$

For the dominant (real) behaviour for large s we have agreement between the two sides

of (3.17) using completeness

$$\sum_n \phi_n^{a\bar{b}}(x)\phi_n^{a\bar{b}}(x') = \delta(x-x'). \tag{3.18}$$

For the imaginary part we have for the left-hand side

$$-\pi\delta(x-x')\delta\left(s-\frac{m_a^2}{x}-\frac{m_b^2}{1-x}\right) \approx -\frac{\pi}{s}\left[\frac{m_a^2}{s}\delta(x)\delta(x')+\frac{m_b^2}{s}\delta(x-1)\delta(x'-1)\right] \tag{3.19}$$

while for the right-hand side we have

$$-\pi\sum_n \phi_n^{a\bar{b}}(x)\phi_n^{a\bar{b}}(x')\delta(q^2-m_n^2) \approx -\frac{1}{\pi m^2}\phi_n^{a\bar{b}}(x)\phi_n^{a\bar{b}}(x'). \tag{3.20}$$

We observe from (3.8) that when $\phi_n(x)$ is integrated against a smooth function it essentially has the behaviour

$$\phi_n^{a\bar{b}}(x) \approx \frac{1}{\pi n}\left[\frac{m_a}{m}\delta(x)+(-1)^n\frac{m_b}{m}\delta(x-1)\right]. \tag{3.21}$$

Substituting (3.21) in (3.20) one finds consistency with (3.19). We thus see in a very concrete manner how confined quarks act as if they were free. However, Eq. (3.21) is a reasonable approximation only if Eq. (3.17) is being integrated against a smoothly varying function. This will turn out *not* to be the case in naive parton model applications involving quark fragmentations and a different analysis will be required there.

3.2. The parton model and processes involving long distances

The processes discussed above are controlled by short-distance phenomena: the colliding e^+e^- create a $q\bar{q}$ pair in a very small volume or the electron in deep inelastic scattering probes the target at very short distances. The final state which emerges is changed from a $q\bar{q}$ pair to a meson by confinement but on the average this final state interaction does not change the probability for the process to take place.

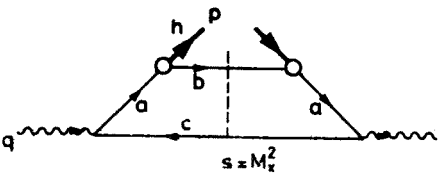

Fig. 20. "Crossed handbag" diagram for $\gamma^* \to hX$

Consider on the other hand the single-particle inclusive annihilation cross-section ($e^+e^- \to \gamma^* \to hX$). In the parton model this is usually represented by the "crossed handbag" diagram analogous to Fig. 15a — see Fig. 20. However, in this case such a diagram cannot represent the impulse approximation as it does for deep inelastic scattering. The meson h emerges only after the confining interaction has had a long time to interact — the quark a does not propagate a short distance. This is particularly evident in QCD_2,

the quarks $a\bar{c}$ resonate to form a (long-lived!) bound state. How can we then calculate this process?

The process $\gamma^* \to hX$ should be related to $\gamma^* h \to X$ by analytic continuation. If we take the virtual Compton amplitude $\gamma^* h \to \gamma^* h$ whose imaginary part gives the deep inelastic total cross-section and continue one q^2 to a positive value $+i\varepsilon$ and the other to a positive value $-i\varepsilon$ meanwhile crossing the meson lines we obtain an amplitude whose imaginary part gives the desired annihilation single-particle inclusive cross-section. If this continuation can also be applied to the scaling function (Eq. (3.15)) in the scaling region, it corresponds to

$$x_B \to \frac{1}{x_F} \pm i\varepsilon, \tag{3.22}$$

where $x_F \equiv p_-/q_-$ is the usual Feynman momentum fraction of the produced hadron and the $\pm i\varepsilon$ depend upon which q^2 enters in x_B. Therefore, although no general proof has ever been given, we expect $\gamma^* \to hX$ to be given by the analytic continuation of Eq. (3.15) in the scaling region. Since $0 \leqslant x_F \leqslant 1$, this analytic continuation takes x_B to values greater than 1. We need therefore the analytic continuation of the wave function to argument greater than unity. Let us call the continued wave function $\Phi_h^{a\bar{b}}(z)$. Then we expect for annihilation

$$\text{Im } A_{--} = (q_- - p_-)^2 \frac{4\pi m_c^2 e_{ac}^2}{s^2} \left| \Phi_h^{a\bar{b}}\left(\frac{1}{x_F}\right) \right|^2. \tag{3.23}$$

Since $\phi(x)$ has a branch point at $x = 1$ (see (2.27)), $\Phi(1/x_F)$ will be complex. The absolute value arises from the opposite sense of continuation for the two q^2 variables.

In Section 2.5 we described how confinement gave rise to an enhanced probability for finding a quark with $x \approx 1$ and hence the branch point in $\phi(x)$ at $x = 1$ and complexness of $\Phi(x)$ for $x > 1$. Equation (3.23) leads to another ("dual") way of looking at the complexness of Φ [13]: it is due to the presence of meson poles in q^2. Confinement implies the breakdown of the naive parton model picture of Fig. 20 due to the formation of hadronic states in the q^2 channel and these are represented by the phase in Φ. We will discuss this further [13, 27] in Section 4.

We now verify that Eq. (3.23) is indeed the correct result in QCD_2, first in perturbation theory [27] and then in leading order $1/N_c$ [11, 13].

The discontinuity in s of the zeroth order graph is easily computed and is seen to be the analytic continuation ($p_- \to p_-$ and $x_B \to 1/x_F$) of Eq. (3.10). In order g^2 we again have the graphs of Fig. 16. We have again

$$A^{(2a)} = A^{(0)} \Gamma_{ab}^{(2)}\left(p^2, \frac{1}{x_F}\right). \tag{3.24}$$

Now it is important to observe that Eq. (3.24) is *not* the analytic continuation of Eq. (3.11) since as we discussed in Section 2.4, $\Gamma^{(2)}$ for x in [0, 1] is not related to $\Gamma^{(2)}$ for $x \geqslant 1$ due to the principal value in Eq. (2.30). The amplitude $A^{(2b)}$ contains a piece which blows up like $q^4 A^{(0)}$. However, this cancels against a similar term from the time-ordering of $A^{(2c)}$

analogous to $A^{(2c_2)}$ leaving a scaling contribution

$$A^{(0)}\left(i\pi m^2 \frac{d}{dx}\frac{1}{p^2-H_0^{ab}(x)}\bigg|_{x=1/x_F}\right). \tag{3.25}$$

The sum of (3.24) and (3.25) is in fact just the analytic continuation of (3.11) from x inside [0, 1] to $x > 1$. As expected, therefore, the contribution of interactions between quarks a and $\bar{c}$ (Fig. 16b) and b and $\bar{c}$ (Fig. 16c) is not negligible in this case and in fact gives rise to an imaginary part in the wave function (3.13) in this order. This is indicative of what happens non-perturbatively in leading order $1/N_c$.

In leading order $1/N_c$ the state X is a single meson state which we label n and thus

$$\text{Im}\, A_{--} \approx \frac{1}{\pi m^2}|F_-|^2. \tag{3.26}$$

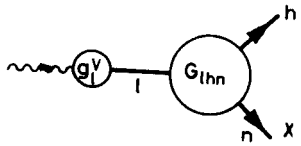

Fig. 21. Meson inelastic form factor, F_- (Eq. (3.27))

The inelastic meson form factor F_- is given in terms of a sum over meson poles at m_l^2 by (see Fig. 21)

$$F_- = q_- \sum_{l=1}^{\infty} \frac{m^2 g_l^V G_{hnl}}{q^2-m_l^2+i\varepsilon}, \tag{3.27}$$

where g_l^V is the photon-meson coupling given in Eq. (3.7) and G_{hnl} is the three-meson coupling [8, 17, 23]:

$$G_{hnl} = \sqrt{\frac{\pi}{N_c}}\, 2m^2 \frac{p_-}{q_- - p_-}\int_0^1 dx \int_0^1 dx' \frac{\phi_h^{b\bar{a}}(x)\phi_n^{c\bar{b}}(1-x')}{[x(p_-/(q_- - p_-))+x']^2}$$

$$\times\left[\phi_l^{c\bar{a}}\left(\frac{1-x'}{q_-/(q_- - p_-)}\right) - \phi_l^{c\bar{a}}\left(\frac{1+x(p_-/(q_- - p_-))}{q_-/(q_- - p_-)}\right)\right]. \tag{3.28}$$

In the limit of interest the dominant contribution comes from $m_l^2 \approx q^2$ where

$$\sum_{l=1}^{\infty} \frac{1}{q^2-m_l^2+i\varepsilon} \to \frac{1}{\pi^2 m^2}\int_0^{\infty} \frac{d\lambda}{1-\lambda+i\varepsilon}.$$

In this case the wave functions ϕ_l and ϕ_n oscillate rapidly. Only the first term in (3.28) survives since in it the oscillations in x' are in phase (in $\phi_n^{c\bar{b}}(-x')$ the separation of nodes

in x' is $\sim 1/n \propto 1/s$ while in $\phi_l^{c\bar{a}}(1-x'/(q_-/(q_- - p_-)))$ it is $(1/l)\cdot(q_-/(q_- - p_-)) \propto 1/q^2(q^2/s) = 1/s$). Using (3.9) we obtain [31]

$$F_- \sim \frac{(q_- - p_-)}{s}\,\frac{2mm_c e^{ac}}{\pi}\left(1-\frac{1}{x_F}\right)\int_0^1 dz\int_0^1 du\int_0^\infty \frac{d\lambda}{\lambda(1-\lambda+i\varepsilon)}$$

$$\times \frac{\phi_h^{a\bar{b}}(u)}{\left[(1-u)^2+\dfrac{(1-x_F)}{x_F}(1-z)\right]^2}\,\phi_n^{c\bar{b}}(z)\phi_l^{c\bar{a}}((1-x_F)z). \tag{3.29}$$

The dominant contribution of the product of the two final coherent wave functions is given by the cosine of their phase difference. From Eq. (2.24) one has

$$\phi_n^{c\bar{b}}(z)\phi_l^{c\bar{a}}((1-x_F)z) \approx \cos\frac{1}{\pi m^2}\left\{m_n^2(1-\lambda)z+\tilde{m}_c^2\ln\lambda - m_h^2\frac{(1-x_F)}{x_F}z\right.$$

$$\left.-\tilde{m}_a^2\ln\left[1-(1-x_F)z\right]+\tilde{m}_b^2\ln(1-z)\right\}. \tag{3.30}$$

The λ contour can be extended to minus infinity in (3.29) then closed in the appropriate half-plane for each of the two exponentials in the cosine in (3.30). We find after a change of variables [11, 13]

$$F_- \sim \frac{(q_- - p_-)}{s}\,2\pi mm_c e^{ac}\left[\frac{i}{\pi}\int_1^{1/x_F} dw\int_0^1 du\,\frac{\phi_h^{a\bar{b}}(u)}{(u-w)^2}\right.$$

$$\left.\times\exp\left\{-\frac{i}{\pi m^2}\left[-\tilde{m}_a^2\ln x_F w-\tilde{m}_b^2\frac{1-\dfrac{1}{x_F}}{1-w}-m_h^2\left(\frac{1}{x_F}-w\right)\right]\right\}\right]. \tag{3.31}$$

It can be shown [11, 13] rather easily using 't Hooft's equation that the quantity in brackets is precisely the analytic continuation $\Phi_h^{ab}(1/x_F)$ of $\phi_h^{ab}(x)$. Thus (3.26) plus (3.31) verifies the expected result of analytic continuation (3.23).

The scaling law of Eq. (3.23) is of the form suggested by the parton model "crossed handbag" diagram (Fig. 20). The quantity $|\Phi_h^{ab}(1/x_F)|^2$ could be interpreted as the probability of quark a to fragment into meson h plus quark b since quark c does not enter in it. However, the physics is *not* that of the free propagation of the $a\bar{c}$ pair. The $a\bar{c}$ and $b\bar{c}$ resonances are crucial in obtaining the result (3.23). Here, in contrast to the situation in Section 3.1 (Eqs. (3.7) and (3.16)), in the integral over the wave function ϕ_n of the unobserved state X there are coherent oscillations with the wave function ϕ_l. In this case we *cannot* use the approximation (3.21). All values of x are important. This is a general phenomenon which occurs in the scaling limits of processes where a final state hadron

is involved since it emerges as the result of the decay of a resonance (l in this case). Long-distance effects play an important role giving rise in particular to a complex amplitude Φ.

We now turn to another group of processes which are conventionally described by the parton model: the production of massive lepton pairs in hadron-hadron collisions (Drell-Yan process [32], $h_1h_2 \to \gamma^*X$), the single-particle inclusive spectrum in deep inelastic scattering (Fig. 1, $\gamma^*h_1 \to h_2X$), and the two-particle inclusive spectrum in e^+e^- annihilation ($\gamma^* \to h_1h_2X$). These three processes are again expected to be related by analytic continuation as are the processes ($\gamma^*h \to X$) and ($\gamma^* \to hX$) discussed above. We first discuss the Drell-Yan process since in some sense it is the most basic of the three. Like the process ($\gamma^*h \to X$) it can be expressed in terms of the matrix element of a product of two current at short distances. However, in this case the parton model result (see Fig. 22)

$$A \propto \frac{1}{N_c}(\phi^{a\bar{b}}_{h_1}(x_1)\phi^{c\bar{d}}_{h_2}(x_2))^2, \tag{3.32}$$

where x_1 and x_2 are the momentum fractions of the quarks a and c, respectively, cannot be directly derived from field theory [33] as in the case of deep inelastic scattering due to the unknown energy dependence introduced by the two-hadron state. Said another way, long-distance effects may be important in the evolution of the hadronic matter before the virtual photon is formed.

Let us first examine the Drell-Yan process in QCD_2 in perturbation theory [27] where as usual the hadrons are replaced by $(-)$ components of vector currents. In zeroth

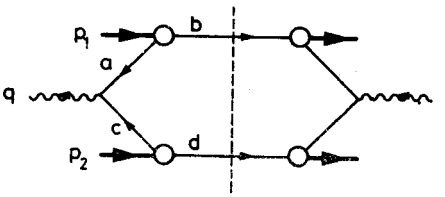

Fig. 22. Parton model diagram for the Drell-Yan process

order in g^2 one finds that the diagram of the form of Fig. 22 dominates over bremsstrahlung-type diagrams where the virtual photon is attached to either the b or d quark in Fig. 22. Equation (3.32) holds with ϕ given by Eq. (2.35) with $\Gamma = 1$.

In order g^2 in addition to quark self-mass terms there are graphs like those shown in Fig. 23. The first four graphs cancel amongst themselves leaving only a piece which in turn cancels the quark self-mass terms. The mechanism of this cancellation is the same as that discussed in the case of deep inelastic scattering. The remaining two graphs obviously generate the wave functions in order g^2.

The Drell-Yan formula (3.32) also holds in leading order $1/N_c$ [34]. Thus the parton model result holds even in the presence of confinement in QCD_2. There are two crucial steps in the derivation of the Drell-Yan formula in QCD_2. The first is the use of Fig. 19 (or Eq. (3.21)) which is allowed in this case as the integration is against a slowly varying function – i.e., final state interaction effects are unimportant. The second is the cancel-

lation of contributions (see, e.g., the first graph in Fig. 23) which lead to bound states in the virtual photon channel which in principle are present since the $a\bar{c}$ pair does not propagate freely. The second step does not appear to have such a general basis as the first step. The cancellation arises from the lack of transverse colour charge separation which assures that the deep inelastic parton model result holds [8] (Section 3.1) and also leads to the absence of the Pomeron in QCD_2 [17, 18]. Since in four dimensions we expect the first result to still hold but not the second, it is not obvious what will happen in the Drell-Yan process [35].

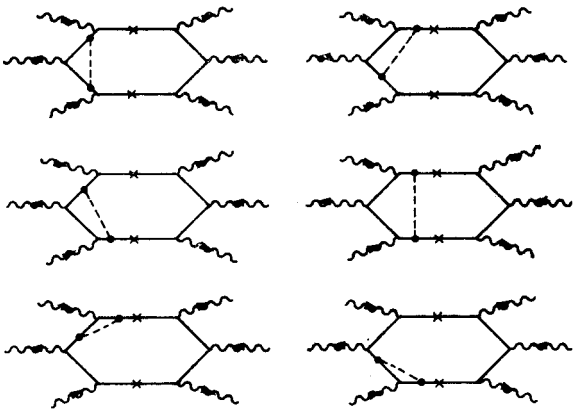

Fig. 23. Model Drell-Yan amplitudes in $O(g^2)$

The naive parton model graph for the deep inelastic single-particle inclusive cross-section ($\gamma^* h_1 \to h_2 X$) is obtained from Fig. 22 by crossing (see also Fig. 1). The kinematics is conveniently described in the Breit frame where the momenta (E, p) are:

$$h_1 : \left(P + \frac{m_1^2}{2P},\ -P\right); \quad \gamma^* : (0, 2x_B P). \tag{3.33}$$

The quark a has the momentum before being struck by the virtual photon

$$q_a : (x_B P,\ -x_B P)$$

and after

$$q_c : (x_B P,\ x_B P).$$

The rapidities are then as shown in Fig. 24 [36]. The parton model prediction applies to the region to the right of the "hole" — the photon fragmentation region — and is the analytic continuation of (3.32)

$$A_{--} \propto \left(\frac{q_-}{q^2}\right)^2 \frac{1}{N_c} \left|\tilde{\phi}_{h_1}^{a\bar{b}}(x_B) \Phi_{h_2}^{c\bar{d}}\left(\frac{1}{x_F}\right)\right|^2 \tag{3.34}$$

where

$$x_F \equiv p_{2-}/(p_{1-}+q_-). \tag{3.35}$$

The behaviour in the remaining part of the rapidity plot is related to soft hadronic effects and is thus more complicated.

In this process confinement again plays an essential role. The $b\bar{c}$ system in the direct (s) channel will form bound states leading to a phase which is contained in $\Phi^{c\bar{d}}_{h_2}(1/x_F)$. We

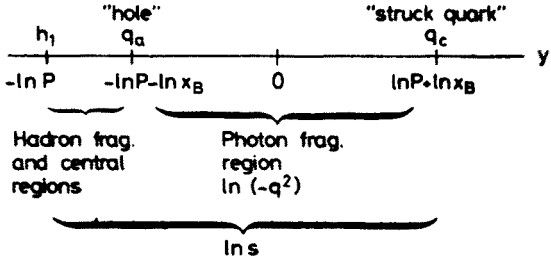

Fig. 24. Rapidity plot for $\gamma^* h_1 \to h_2 X$

have studied this process in QCD_2 in leading order $1/N_c$ [27]. The s channel graphs (Fig. 25a) indeed lead to the parton model formula (3.34). The t channel graphs (Fig. 25b) are negligible when t is large. Since

$$t \approx m_{h_1}^2 x_B + q^2(1-x_F), \tag{3.36}$$

for $1-x_F \approx 1/q^2$, t is finite and these graphs are important and spoil the parton model result. Equation (3.34) also fails for $x_F \approx 1/q^2$, i.e., in the hole fragmentation region.

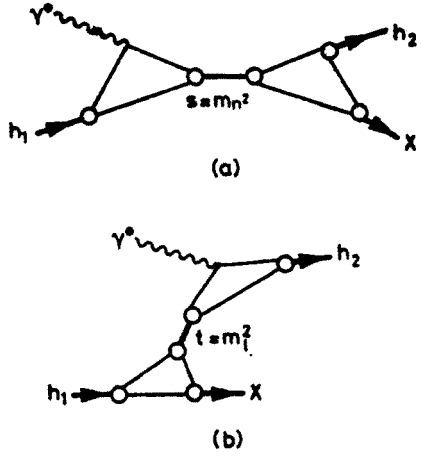

Fig. 25. Bound state contributions to $\gamma^* h_1 \to h_2 X$: (a) s channel bound states; (b) t channel bound states

Equation (3.34) implies a universality of quark fragmentation in annihilation and deep inelastic scattering (at least not too near the edge of the photon fragmentation region in the latter process). The question then arises whether the quark fragmentation function $\propto |\Phi(1/x_F)|^2$ is universal for all processes [17]. We have studied [27] hadron-hadron

scattering ($h_1h_2 \to h_3X$) and we find that although the imaginary part of the amplitude is correctly given by Φ (since it is due to s channel bound states) the real part is not. Hence quark fragmentation is *not* universal. We expect to obtain the distribution $|\Phi(1/x_F)|^2$ only in situations where all invariants are large. Otherwise, exchange (t channel) effects become important as we saw in the case of $\gamma^*h_1 \to h_2X$.

4. Confinement and the parton model

In this section, motivated by the QCD_2 results discussed in Section 3, I discuss some consequences which confinement may have for applications of the naive parton model. We saw in Section 3 that (within some limitations to be discussed below) in QCD_2 scaling laws of the form suggested by the naive parton model of freely propagating quarks held for all processes involving a large q^2 (spacelike or timelike) current. I believe this is strong support for the parton model predictions.

The fact that the naive parton model predictions are true in QCD_2 is not a trivial result. They are true even though the parton model picture of freely propagating quarks does not generally hold. In processes involving quark fragmentation the observed hadron emerges at long times after the occurrence of the basic hard subprocesses. Confinement leads to the formation of hadronic intermediate states (compare, e.g., Figs. 20 and 21) and a characteristic imaginary part to the amplitude in the scaling limit. We explicitly verified that, nevertheless, scaling laws of the same form suggested by the parton model held. Although one suspects there is some basic physics of the hadronic states which leads to this rather remarkable result (in particular, the lack of dependence on the non-fragmenting quark) we have not yet been able to discover it. The validity of the scaling laws can be understood in another, more mathematical, way, however. If one considers a crossed process where the produced final state hadron now becomes an initial hadron (e.g., $\gamma^* \to hX$ to $\gamma^*h \to X$ or $\gamma^*h_1 \to h_2X$ to $h_1h_2 \to \gamma^*X$) the hadronic intermediate states are now in a momentum transfer channel and are unimportant. The parton model scaling laws for the crossed process then imply, through analyticity, parton model scaling laws for the original process involving quark fragmentation. This is expected to be true in any theory. We might say then that in a confining theory: "the parton model is the scaling laws due to light-cone dominance plus analyticity".

The validity of the parton model scaling laws in QCD_2 is non-trivial in another respect. Although the parton model for deep inelastic scattering follows directly from the short-distance behaviour of the theory (and the procedure of averaging over the hadronic singularities – Fig. 19), this is not the case for the Drell-Yan process. We saw that a special cancellation must also take place to remove the effect of the hadronic states in the virtual photon channel. If this cancellation had not occurred, the Drell-Yan process would have been of order N_c^0 rather than the conventional N_c^{-1} in the $1/N_c$ expansion [34]. Since this cancellation is related to other cancellations in QCD_2 some of which are expected to generalize to four-dimensions and some not, it is difficult to assess its generality. Nonetheless, I feel that the QCD_2 results are support for the compatibility of confinement and the Drell-Yan parton model prediction for massive lepton pair production.

One of the important features of the parton model is the universality of the quark fragmentation function. We found universality to hold in QCD_2 in those instances where all the channel invariants are large. This seems like a very natural limitation since if some channel invariant is small (typically for an exchange channel), then bound states in that channel (or Regge exchanges, etc.) can become important and destroy the parton model predictions. Thus, in particular, the single-particle inclusive spectrum in hadron-hadron collisions at small momentum transfer cannot be expected to be given by the quark fragmentation function which occurs in e^+e^- annihilation and deep inelastic scattering. In addition the failure of universality may imply a breakdown of the Bjorken-Kogut correspondence arguments [37] in some cases [27].

We discussed in Sections 2 and 3 one special feature of the hadron and quark fragmentation functions of QCD_2 which appears to be a general consequence of confinement. We noted above that confinement leads to the formation of hadronic intermediate states in processes involving quark fragmentation which give a characteristic phase to the quark fragmentation amplitude (Φ of Section 3.2). On the other hand, we saw in Section 2.5 how the long-range confining force led to an enhanced amplitude for finding a wee quark in a meson compared to the usual behaviour in a superrenormalizable theory and hence singularities in the meson-quark-antiquark wave function in the quark mass variable x at $x = 0$ (and $x = 1$): $\phi_h^{a\bar{b}}(x) \sim x^{\beta_a}$, $(1-x)^{\beta_b}$ with $0 \leqslant \beta_i \leqslant 1$. This wave function gives the hadron fragmentation function measurable in deep inelastic scattering. Due to the branch points in $\phi(x)$ at $x = 0,1$ its analytic continuation $\Phi(x)$ which gives the quark fragmentation function measurable in e^+e^- annihilation is complex. There is therefore an amusing duality between the quark-parton and hadron interpretations of this phase [13]. While in non-confining theories the singularities in the hadronic channels referred to above are not present and no phase is required, in confining theories they cannot be neglected and we expect the continued wave function to be complex. We therefore believe that the existence of singularities in $\phi(x)$ at $x = 0,1$ may be a very general feature of confinement.

The existence of a singularity in $\phi(x)$ at $x = 1$ implies via the Drell-Yan-West relation a violation of the integral asymptotic power behaviour of form factors as predicted by dimensional counting [15, 38]. In QCD_2 explicit calculation confirms this [8]: $F(q^2) \sim (q^2)^{-1-\beta}$. The form factor decreases less rapidly than is the case in a non-confining superrenormalizable theory ($F(q^2) \sim (q^2)^{-2}$) due to the enhanced probability of finding "wee" quarks in a meson. The origin of the large q^2 behaviour of the form factor is quite different [8] from that envisaged in renormalizable theories [15] where $F(q^2) \sim (q^2)^{-1}$. The phase in Φ could also lead to interference effects in annihilation and deep inelastic scattering [27, 39]. If one takes the small value of β for light quarks in QCD_2 [5, 8] seriously, these effects may be hard to detect experimentally. Nonetheless, they should be kept in mind since they are likely consequences of confinement and may be important especially for heavy quarks.

Above, I have tried to abstract some possible consequences of long-distance (confinement) effects for the parton model from the explicit results obtained in QCD_2. As noted in Section 1, one hopes that the long-distance effects (confinement) and the short-distance effects (asymptotic freedom) can be treated rather independently and their effects combined

at the end to give an improved parton model [40]. Studies in QCD_2 unfortunately cannot give any definitive answer to whether or not his hope is realized since there is exact scaling and no short-distance modifications of the naive parton model results. Although nothing in QCD_2 is in direct contradiction with this assumption, the important role played by hadronic bound states in processes with quark fragmentation raises a possible question about the factorization of the short-distance and long-distance effects in these processes.

The results discussed here are only a beginning attempt to explore the relationship between the parton model and confinement. A complete understanding will have to await a more complete and practical understanding of confinement in QCD_4.

These lectures are based mostly on work done with R. Anishetty, M. Baker, R. C. Brower and W. L. Spence. I am greatly indebted to them for many illuminating discussions. I would also like to thank S. D. Ellis, C. Sachrajda, G. Veneziano and T. T. Wu for discussions.

APPENDIX

Gauge invariance

All studies of physical processes in QCD_2 have so far been carried out using the light-cone gauge formalism discussed in Section 2. Since physical amplitudes are gauge invariant, we would expect to obtain the same result in any other gauge. However, doubts have been raised in the literature about the behaviour of QCD_2 in other gauges, specifically the axial gauges ($\eta \cdot A = 0$, η any vector).

Frishman et al. [41] some time ago pointed out some difficulties with the integral equations for the quark self-energy and the quark-antiquark scattering amplitude in axial gauges other than the light-cone gauge. These problems have recently been resolved by Bars and Green [42] and from their work there appears to be nothing internally inconsistent in axial gauges using the principal value prescription to regulate the gluon singularity. Bars and Green did not attempt to show that physical colour singlet amplitudes were gauge invariant.

On the surface it would appear that one could show gauge invariance through use of the Ward identities analogously to what is done in four dimensions [43, 44]. Indeed one can just take the Feynman rules for four-dimensional QCD and specialize them to two dimensions. The gluon propagator in the axial gauge $\eta \cdot A = 0$ is

$$D_{\mu\nu}^{ab} = \frac{i\delta^{ab}}{k^2}\left[g_{\mu\nu} - \frac{k_\mu\eta_\nu + \eta_\mu k_\nu}{\eta \cdot k} + \eta^2 \frac{k_\mu k_\nu}{(\eta \cdot k)^2}\right], \tag{A1}$$

where the $\eta \cdot k$ singularities are regulated by taking the principal value and there are no ghosts. When the three and four gluon vertices are multiplied by gluon propagators (A1) on all legs they vanish in two dimensions. Thus in QCD_2 we can also include graphs with three and four gluon vertices since they contribute nothing. Under a change in gauge $\eta \to \eta + \delta\eta$, one easily sees that $\delta D_{\mu\nu}$ is proportional to k_μ and/or k_ν. The change in an amplitude is thus proportional to the divergence of an amplitude with two external gluons.

It would appear then that the Ward identities could be used as is usually done in QCD_4 [45] to show this divergence vanishes and hence the amplitude is gauge invariant [44].

Wu [46] has pointed out recently, however, that such an application of the Ward identities is too naive due to the very strong singularities in the gluon propagator ((2.5) and (A1)). The Ward identities seem to show that the numerators of various Feynman integrals vanish, but due to the singularities in the denominators if one evaluates each integral and adds them up one does not find zero. This problem occurs only in graphs with

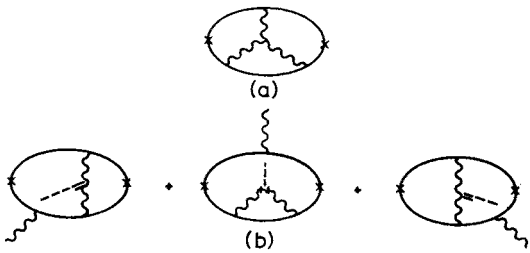

Fig. A.1. (a) A three-gluon vertex contribution to the two-point function. (b) Contributions arising from (a) under a change of gauge $\eta \to \eta + \delta\eta$. The dashed lines indicate k_μ applied to a gluon line

two or more gluon propagators where there is more than one principal value involved so let us illustrate it with the simplest example: the two-point function in $O(g^4)$. According to the scheme outlined above we include also graphs with a three-gluon vertex, for example Fig. A.1a. Under a small change $\eta \to \eta + \delta\eta$ any one of the three gluon propagators may change leading contributions like those shown in Fig. A.1b to leading order in $1/N_c$.

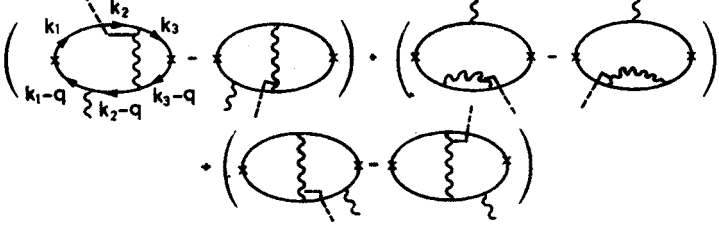

Fig. A.2. Contributions to the change of the two-point function under $\eta \to \eta + \delta\eta$ which are related to Fig. A.1b

Normally these would be combined with the six contributions in Fig. A.2 to give zero using the Ward identities. Note some terms are dropped because they are non-leading in $1/N_c$.

The introduction of the graphs of Fig. A.1 is just a trick to organize the graphs which should combine to cancel. Since the change in the amplitude without them (e.g., Fig. A.2) should vanish [43, 46] we should have found that the sum in Fig. A.1b as well as that in Fig. A.2 should vanish. This is indeed the case for the sum of Fig. A.1b but is not for

that of Fig. A.2. Adding on six similar graphs inverted top to bottom we find for a small change of gauge away from the light-cone gauge the sum is proportional to

$$\int_0^1 dx_1 \int_0^1 dx_2 \int_0^1 dx_3 \frac{1}{q^2 - H_0(x_1)} \frac{1}{q^2 - H_0(x_3)}$$

$$\times \left[\frac{1}{(x_1 - x_2)^3} \left(\frac{1}{(x_2 - x_3)^2} - \frac{1}{(x_3 - x_1)^2} \right) + \text{cyclic perms.} \right], \tag{A2}$$

where $x_i = k_i/q_-$ and q is the external momentum. The quantity in square brackets can be written as [46]

$$-\tfrac{1}{2} \frac{\partial^3}{\partial x_1 \partial x_2 \partial x_3} \left[\frac{1}{(x_1 - x_2)} \frac{1}{(x_2 - x_3)} + \frac{1}{(x_2 - x_3)} \frac{1}{(x_3 - x_1)} + \frac{1}{(x_3 - x_1)} \frac{1}{(x_1 - x_2)} \right]. \tag{A3}$$

If one disregards the $\pm i\varepsilon$'s, the brackets in Eq. (A3) vanish. However, if each denominator is a principal value denominator, one finds

$$-\frac{\varepsilon^2}{2} \frac{(x_1 - x_2)^2 + (x_2 - x_3)^2 + (x_3 - x_1)^2}{[(x_1 - x_2)^2 + \varepsilon^2][(x_2 - x_3)^2 + \varepsilon^2][(x_3 - x_1)^2 + \varepsilon^2]}. \tag{A4}$$

Although this is apparently of order ε^2, it gives rise to a finite contribution to Eq. (A2) from the region of integration $(x_i - x_j) = O(\varepsilon)$. (Note the x_2 integration can be done trivially so the integration volume is $O(\varepsilon^2)$ while Eq. (A4) is $O(\varepsilon^{-2})$.) A similar argument applies to the remaining contributions to the change in the amplitude. Thus the naive gauge invariance agreement apparently fails [46]. Wu has consequently advocated abandoning the principal value prescription (2.5). He has introduced a new regularization prescription which preserves gauge invariance. Unfortunately this leads to a very complicated equation for the bound states which has resisted solution [47].

However, the issue is not fully resolved yet. The above criticism of the ordinary principal value prescription is not watertight; the problem is riddled with singularities. It is possible that the ordinary principal value prescription in the light-cone gauge gives the correct *physical* amplitudes for external colour singlet sources.

Some weak points in the above criticism are the following.

(*i*) Wu used the form

$$D_{\mu\nu}^{ab} = i\delta^{ab} \frac{\eta_{\perp\mu}\eta_{\perp\nu}}{(\eta \cdot k)^2}, \tag{A5}$$

where $\eta \cdot \eta_\perp = 0$, for the gluon propagator. For this form, it is not true that $\delta D_{\mu\nu}/\delta\eta$ is proportional to k_μ since $P(1/x^2) \neq xP(1/x^3)$ for such singular integrals encountered here. Thus the change in the amplitude is not actually given by Fig. A.2 or Eq. (A2). The choice of propagator in Eq. (A1) presents other difficulties – the $1/k^2$ singularity must be regularized though it is spurious in two dimensions. In fact one cannot pass to the principal value light-cone gauge using Eq. (A1) [44].

(*ii*) Infinities appear in the change of the amplitude $\delta A/\delta\eta$ when the above procedure is used which do not appear in the amplitude in a given gauge. For a change away from the light-cone gauge the k_+ integrals become ultra-violet divergent [48].

I believe the gauge invariance problem needs further study in order to resolve these points. What would be useful are some simple explicit calculations of *physical* amplitudes in two different gauges using the principal value prescription like (2.5) and using Wu prescription [46]. Any disagreement between the results would then eliminate once and for all some prescriptions.

The Ward identities can also be used to show formally that the $1/(\eta \cdot k)^2$ gluon propagator cancels in the sum of all graphs contributing to a physical amplitude [44, 49]. This would then seem to provide an understanding of the reason why the principal value prescription does not spoil analyticity of physical amplitudes [14]. Unfortunately this argument suffers also from similar difficulties to the gauge invariant argument.

This being the "state of the art", in these lectures I have discussed QCD_2 as originally formulated by 't Hooft. It is possible that it gives the correct physical amplitudes for a gauge invariant two-dimensional QCD. Even if it does not, as long as it has no internal inconsistencies, it is a model with both confinement and partons and is therefore, I think, very interesting. One can see from the results of Section 2 and Section 3.1 that the model so far has exhibited no internal inconsistencies. On the contrary, the verification of Eq. (3.3) demonstrates a high degree of consistency between the unambiguous perturbation theory graph of Fig. 12 and the solutions of 't Hooft's equation (Eq. 3.8)).

Editorial note. This article was proofread by the editors only, not by the author.

REFERENCES AND FOOTNOTES

[1] R. P. Feynman, *Photon-Hadron Interactions*, Benjamin, Reading 1972.

[2] For a discussion of current models and further references, see M. J. Teper, Rutherford Preprint RL–78–022/A (1978).

[3] J. C. Polkinghorne, *Acta Phys Pol.* **B9**, 1025 (1978); D. A. Ross, T.–M. Yan, *Acta Phys. Pol.* to be published.

[4] G. 'tHooft, *Nucl. Phys.* **B75**, 461 (1974).

[5] J. Ellis, *Acta Phys. Pol.* **B8**, 1019 (1977).

[6] G. t'Hooft, *Nucl. Phys.* **B72**, 461 (1974).

[7] G. Veneziano, *Nucl. Phys.* **B117**, 519 (1976).

[8] M. B. Einhorn, *Phys. Rev.* **D14**, 3451 (1976).

[9] S. Coleman, unpublished, referred to in Ref. [8].

[10] P. Federbush, A. Tromba, *Phys. Rev.* **D15**, 2913 (1977); S. Hildebrandt, V. Višnjić, *Phys. Rev.* **D17**, 1618 (1978) and to be published.

[11] R. C. Brower, W. L. Spence, J. H. Weis, to be published.

[12] S.–S. Shei, H.–S. Tsao, IAS Preprint (1977), have independently observed this analogy.

[13] R. C. Brower, W. L. Spence, J. H. Weis, *Phys. Rev. Lett.* **40**, 674 (1978).

[14] R. C. Brower, W. L. Spence, J. H. Weis, *Phys. Rev.* to be published.

[15] S. J. Brodsky, G. Farrar, *Phys. Rev. Lett.* **31**, 1153 (1973); V. A. Matveev, R. M. Muradyan, A. N. Tavkhelidze, *Nuovo Cimento Lett.* 7, 719 (1973); R. Blankenbecler, S. J. Brodsky, *Phys. Rev.* **D10**, 2973 (1974).

[16] K. Johnson, *Phys. Rev.* **D6**, 1101 (1972).

[17] R. C. Brower, J. Ellis, M. G. Schmidt, J. H. Weis, *Phys. Lett.* **65B**, 249 (1976); *Nucl. Phys.* **B128**, 131, 175 (1977).
[18] M. B. Einhorn, S. Nussinov, E. Rabinovici, *Phys. Rev.* **D15**, 2282 (1977); M. B. Einhorn, E. Rabinovici, *Nucl. Phys.* **B128**, 421 (1977).
[19] It is appropriate to choose the $(-)$ component of a vector current since in a bound state wave function the external quark lines always interact through a gluon exchange which implies a factor γ_- adjacent to each quark propagator. To obtain an amplitude analogous to the meson amplitude, a factor $(\sqrt{N/\pi}\,)p_i$ should be extracted for each external line — see below Eq. (2.11).
[20] See, e. g., L. Bertocchi, S. Fubini, M. Tonin, *Nuovo Cimento* **25**, 626 (1962); D. Amati, A. Stanghellini, S. Fubini, *Nuovo Cimento* **26**, 6 (1962); V. N. Gribov, ITEF Summer School Lectures, Vol. I, 65 (1973).
[21] Quark loops in higher orders of $1/N_c$ are expected to modify Eq. (2.37) through t channel iterations of purely mesonic amplitudes. Since these iterations have a multiperipheral structure, perhaps one should say that the input amplitudes for the multiperipheral model have a characteristic behaviour in confining theories.
[22] J. Randa, Manchester University Preprint (1977).
[23] C. G. Callan, N. Coote, D. J. Gross, *Phys. Rev.* **D13**, 1649 (1976).
[24] E. Poggio, H. Quinn, S. Weinberg, *Phys. Rev.* **D13**, 1958 (1976).
[25] R. Shankar, *Phys. Rev.* **D15**, 755 (1977).
[26] We have ignored a delicate point in the above discussion. Presumably (3.2) is not valid very close to the real axis ($\theta \approx 0, 2\pi$). For example, as Q_2^2 changes so as to pass a bound state the sum changes discontinuously. We assume that this effect can be made small by including a sufficiently large number of bound states in (3.6).
[27] R. Anishetty, R. C. Brower, W. L. Spence, J. H. Weis, to be published.
[28] The reader may have remarked that the scaling behaviours (3.3) and (3.10) seem to differ from the canonical behaviours in four dimensions. However, this is just a reflection of the fact that there are only longitudinal photons in two dimensions. The apparently unusual scaling behaviours are irrelevant as concerns what we want to abstract from the model. (I thank W. L. Spence for emphasizing this point to me.)
[29] The same mechanism is responsible for the absence of the Pomeron in QCD_2 (Refs. [17] and [18]). We return to this point below.
[30] There are additional contributions analogous to $A^{(2b)}$ and $A^{(2c_1)}$ which cancel between themselves (Ref. [8]).
[31] M. B. Einhorn, *Phys. Rev.* **D15**, 3037 (1977).
[32] S. D. Drell, T. M. Yan, *Phys. Rev. Lett.* **25**, 316 (1970).
[33] R. L. Jaffe, *Phys. Rev.* **D5**, 2622 (1972).
[34] J. Kripfganz, M. G. Schmidt, *Nucl. Phys.* **B125**, 323 (1977).
[35] Any naive introduction of transverse momenta destroys the cancellation in all three cases and is thus not an acceptable model.
[36] J. D. Bjorken, *Phys. Rev.* **D7**, 282 (1973).
[37] J. D. Bjorken, J. Kogut, *Phys. Rev.* **D8**, 1341 (1973); J. Kogut, *Phys. Rev.* **D8**, 3029 (1973).
[38] We should note that a logarithmic singularity would not be inconsistent with dimensional counting, however.
[39] We thank S. Brodsky for discussions on this point.
[40] For example, the results of a confinement model might be taken to give the parton distributions at some Q^2 which then change with Q^2 according to the predictions of asymptotic freedom.
[41] Y. Frishman, C. T. Sachrajda, H. Abarbanel, R. Blankenbecler, *Phys. Rev.* **D15**, 2275 (1977).
[42] I. Bars, M. B. Green, *Phys. Rev.* **D17**, 537 (1978).
[43] C. T. Sachrajda, unpublished.
[44] R. Anichetty, M. Baker, J. H. Weis, University of Washington Preprint RLO-1388-750 (1978), unpublished.

[45] G. 'tHooft, M. Veltman, in *Particle Interactions at Very High Energies*, Part B, Ed. by F. Halzen et al., Plenum, New York 1974; W. Konetschny, W. Kummer, *Nucl. Phys.* **B100**, 1061 (1975); **B108**, 397 (1976); A. Sugamoto, H. Yamamoto, N. Nakagawa, to be published.
[46] T. T. Wu, *Phys. Lett.* **71B**, 142 (1977) and to be published.
[47] See, however, N. J. Bee, P. J. Stopford, B. R. Webber, Cambridge Preprint (1978).
[48] Symmetric integration was adopted in obtaining (A2). Explicit calculation shows that (A2) is finite and the remaining graphs not included in (A2) are infinite indicating gauge non-invariance. However, this ignores point (*i*) and possible ambiguities due to (*ii*).
[49] C. Handy, Columbia University Preprint (1978).